Journal of Translational Medicine

RESEARCH

Open Access

# Clinical outcomes of autologous adipose-derived mesenchymal stem cell combined with high tibial osteotomy for knee osteoarthritis are correlated with stem cell stemness and senescence

Houyi Sun[1†], Haoxin Zhai[1†], Kaifei Han[1,4†], Heran Ma[2], Yi Tan[2], Shihao Li[1], Zhicheng Liu[1], Lei Cheng[1], Qunshan Lu[1*], Libo Zhou[3*] and Peilai Liu[1*]

## Abstract

**Background** Mesenchymal stem cells (MSCs) have been proposed to treat osteoarthritis (OA) for many years. However, clinical outcomes have been inconsistent due to biological variation between patients, differences in tissue source and preparation of the MSCs, and type of donor (e.g. allogenic versus autologous). Here, we test the hypothesis that inconsistent clinical outcomes are related to variations in the stemness and senescence of the injected autologous adipose-derived (AD) MSCs.

**Methods** In the prospective randomized trial, 45 knee OA patients were divided into two groups: Group 1 (n = 22) patients treated with high tibial osteotomy (HTO) alone and Group 2 (n = 23) patients treated with HTO followed by intra-articular injection of autologous AD-MSCs (HTO + AD-MSCs). MRI and X-ray were performed pre-operation and 12 months post-operation. WOMAC and VAS score were collected four times, every 6 months over a 24-month follow-up. We observed the proliferation and stemness of AD-MSCs selected from the 5 patients showing the most improvement and from the 5 patients with the least improvement, and completed further in vitro experiments including beta-galactosidase activity, reactive oxygen species and bioinformatic analysis.

**Results** The results showed that patients treated with HTO + AD-MSCs had a significant reduction in knee OA severity as compared to patients treated with HTO alone. Moreover, we discovered that proliferation and colony forming efficiency of AD-MSCs selected from the 5 patients showing the most improvement performed significantly better than cells selected from the 5 patients with the least improvement. AD-MSCs from the patients with the most improvement also had lower amounts of senescent cells and intracellular reactive oxygen species.

[†]Houyi Sun, Haoxin Zhai, Kaifei Han contribute equally to this research.

*Correspondence:
Qunshan Lu
luqunshan1112@163.com
Libo Zhou
libozhou@sdu.edu.cn
Peilai Liu
199362000205@email.sdu.edu.cn
Full list of author information is available at the end of the article

**Conclusions** Clinical outcomes of autologous AD-MSCs therapy in knee osteoarthritis are correlated with stem cell stemness and senescence. Our study highlights emerging opportunities and trends in precision medicine that could potentially improve autologous MSC-based therapies.

## Introduction

Osteoarthritis (OA) is a common chronic joint disease characterized by a progressive degeneration of the articular cartilage, which leads to pain, functional impairment, and eventually substantial disability [1, 2]. Non-surgical options for OA remain focused on symptom relief with medications [3, 4], while surgical interventions include procedures such as high tibial osteotomy (HTO) for early-stage OA and total knee arthroplasty (TKA) for advanced cases [5, 6]. Currently, there are very few long-term solutions that repair and regenerate the articular cartilage tissue and address the underlying pathology of OA [7]. As a result, there is an urgent need for new approaches that are able to halt and/or reverse the progression of the disease [8].

Mesenchymal stem cells (MSC) have garnered a lot attention as a "drug store" for treating knee OA due to their ability to secrete trophic factors that have anti-inflammatory and analgesic properties, and as a "cell reservoir" due to their ability to self-renew and differentiate into cells that can repair damaged joint tissue, especially articular cartilage [8, 9]. One additional consideration that makes articular cartilage an attractive site for MSC therapy is safety since the cells are injected locally into the joint as opposed to systemically into the circulation. Over the years, a variety of MSCs from different tissue sources have been used, some with promising results [10]. However, the overall efficacy of MSC-based therapy for OA has been inconsistent [11, 12]. Some studies have reported significant improvements in OA symptoms with MSC-based therapy, while others found no discernible improvement [13–15]. This may be due to differences in individual patients, the source and preparation of the MSCs, as well as allogenic versus autologous donors [16]. In the present study, we hypothesized that the inconsistent clinical outcomes found with autologous MSC-based therapies in OA are related to differences in the quality and quantity of the injected MSCs.

Recently, the concept of MSC "immune privilege" has been challenged due to mounting evidence suggesting that allogenic MSCs elicit an immune response the leads to rejection [17, 18]. Although MSCs produce trophic factors, including transforming growth factor-beta1 (TGF-β1), indoleamine-2,3-dioxygenase (IDO), and prostaglandin $E_2$ ($PGE_2$), which strongly modulate the immune system when MSCs mount a response to an inflammatory environment or are stimulated with interferon-γ (IFN-γ), the stimulated MSCs or their differentiated progeny express high levels of MHC class I and II antigens [19], which delay the rejection of allogeneic MSCs. Moreover, it has been reported that allogeneic MSCs are rejected more quickly in animals that have been previously sensitized, with the majority of the cells killed within 48 h after systemic infusion [20, 21]. Likely, the clinical outcomes of allogeneic MSC therapies are due to the trophic factors produced shortly after infusion, resulting in a so called "hit-and-run" effect [17], while fewer reports have suggested that the newly formed tissue in vivo is generated directly by the transplanted allogeneic MSCs [12, 22]. Biosafety should also be a concern since pathogens, including those known and potentially unknown, can be transmitted from the transplanted allogeneic MSCs to the recipient. Thus, for these reasons, autologous stem cell-based therapies are preferable. In the present study, autologous AD-MSCs were used to treat patients with knee OA because adipose tissue can be isolated from an abundant tissue source via minimally invasive procedures, are functionally comparable to bone marrow (BM)-derived MSCs and pose no immunogenicity risks [23]. Furthermore, AD-MSCs have demonstrated therapeutic efficacy in a variety of diseases, including the repair of critical organs such as the heart, liver, and kidneys, helping to regulate the immune response and tissue repair [24–29]. These multifaceted therapeutic effects underscore the versatility of AD-MSCs and their potential as a valuable cell-based therapy for a wide range of degenerative and inflammatory conditions.

To test our hypothesis, we conducted a prospective randomized controlled trial with 45 knee OA patients who were divided into a control group consisting of 22 patients treated with HTO alone and an experimental group with 23 patients treated with HTO followed by intra-articular injection of autologous AD-MSCs (HTO + AD-MSCs). The effect of treatment was assessed by measuring pain intensity and pain relief, improvement in joint function, and cartilage regeneration in the two groups. Specifically, MRI and X-ray were performed pre-operation and 12 months post-operation. WOMAC and VAS score were collected four times, every 6 months over a 24-month period. More importantly, the characteristics of the injected autologous AD-MSCs were analyzed in the laboratory. The results we obtained supported our hypothesis and, for

the first time, suggest that the stemness and senescence of the injected autologous AD-MSCs were closely correlated with clinical outcomes/success.

## Materials and methods

### Clinical trial design

This clinical study was a prospective, randomized, open-label, blind end point trial conducted at a single institution. All research conducted with human subjects was approved by the Ethics Committee of Qilu Hospital of Shandong University (approval number: 2018-023) and was registered on the U.S. National Institutes of Health sponsored website, www.ClinicalTrials.gov, under the identification number, NCT03955497, before any subjects were enrolled. Informed consent was obtained from all the subjects prior to active participation in the study.

Figure 1A shows a schematic of the experimental design for the study. Initially, 60 knee OA patients were recruited and enrolled; each was provided a subject number that was randomly generated using the PASS (NCSS LLC., USA) software package. After screening to determine if the subjects met the inclusion criteria (Supplemental Table 1), assignment to either the control (n = 22) or experimental (n = 23) groups was performed using a randomization table listing all subject numbers. Inclusion criteria was showed as follows: aged 18–65 years, male and female, patient can tolerate surgery; clinical diagnosis of degenerative arthritis by radiographic criteria; obviously extra-articular malformation; good contralateral interventricular cartilage; course of disease ≥ 6 months; there was no obvious abnormality in tumor marker detection, or patient was evaluated has not at the risk of cancer; subjects who understand and sign the consent form for this study. Exclusion criteria was showed as follows: acute joint injury; patients with severe primary diseases, such as cardiovascular, cerebrovascular, liver, kidney and hematopoietic system, and psychosis; cancer patients; women who are pregnant or breast feeding, or allergic constitution patient; positive serology for hiv-1 or hiv-2, hepatitis b (hbsag, anti-hepatitis c virus -ab), hepatitis c (anti-hepatitis c virus -ab) and syphilis; receive other open surgery related to knee operation within 6 months; participation in another clinical trial; failing to comply with the inclusion criteria, unwilling to comply with the research approach, or incomplete data affecting the curative effect or safety judgment. 15 participants were excluded in this study, among them, 10 patients withdrew, 3 patients had postoperative knee injury and 2 patients were lost to follow-up.

The control group of patients received a medial open-wedge high tibial osteotomy (HTO), while patients in the experimental group received both a HTO and liposuction (used to prepare autologous AD-MSCs) on the day of surgery and then 1 month later received an intra-articular knee injection of $5 \times 10^7$ autologous AD-MSCs (HTO + AD-MSCs). The injected cells were straight from adipose tissue and never frozen. A timeline showing the milestones for the entire 2-year study are shown in Fig. 1B; the milestones include regular examinations to obtain baseline characteristics, HTO surgery, preparation and intra-articular injection of autologous AD-MSCs or vehicle (sodium hyaluronate), and rehabilitation and efficacy evaluation.

### HTO surgery and follow-up protocol

As shown in Fig. 1B, OA patients received preoperative X-rays, an MRI, and laboratory evaluations. All surgical procedures were performed by the same experienced team. For each case, an exploratory arthroscopy was performed immediately before the osteotomy to confirm the indications for a medial open wedge HTO and to evaluate articular cartilage damage. All procedures for performing the medial open wedge HTO were as previously described in detail [30, 31]. In brief, lower limb alignment was carefully adjusted to mild valgus and then fixed using the TomoFix internal fixation system (DePuy Synthes, Switzerland). After the osteotomy was completely healed at 1 year postoperatively, the internal fixation hardware was removed and a second-look arthroscopy performed. All patients received the same physical rehabilitation program and clinical follow-up for at least 2 years (Fig. 1B).

### AD-MSC preparation and injection

To isolate AD-MSCs, 50 ml of autologous adipose tissues of patients were obtained by liposuction from abdominal subcutaneous fat under mature procedures, including sterilization, local anesthesia, incision, injection of tumescent solution, adipose tissue collection, and suture. The adipose tissue was repeatedly rinsed with physiological saline until free of red blood cells, and then incubated with 0.1% type I collagenase (catalog number SCR103, Sigma Aldrich, USA) digestion solution. The sample was sealed and oscillated at 90 revolutions/min for 30–60 min at 37 °C until no large fat particles remained. Cells were collected after removing the fascia with a 100 μm filter and seeded in T75 flask with $3 \times 10^6$ cells/ml, then cultured in a 37 °C and 5% $CO_2$/95% air incubator in MSC Base Medium (catalog number 6114011, Dakewe, China) supplemented with 5% serum substitute (UltroGRO, Helios, USA); media were refreshed 2 times per week. When the cells reached 80% confluency, the cultures were digested using TrypLE solution and serially passaged.

At passage 5 (P5), a series of tests were performed before delivery to the clinic for injection. Before

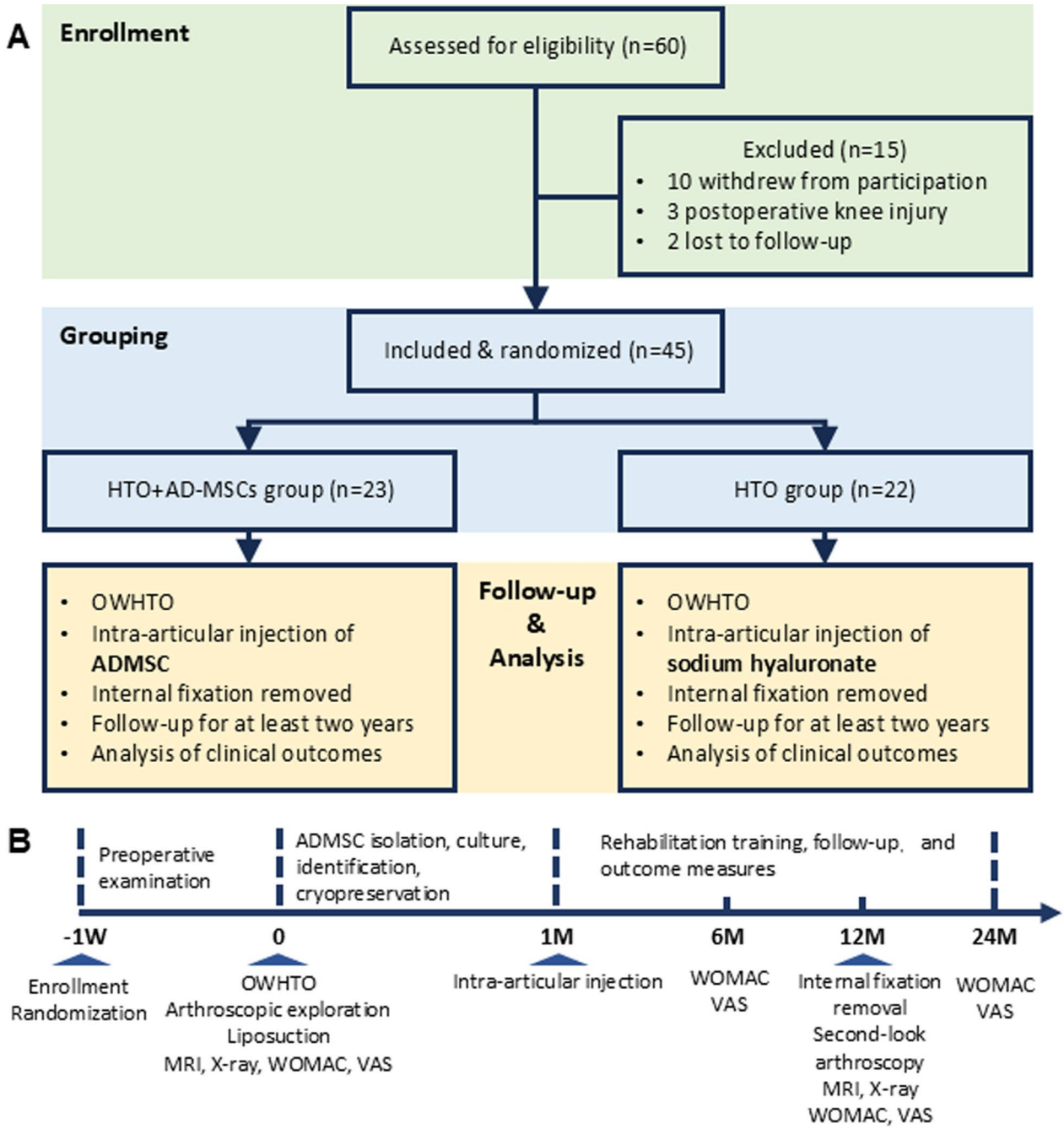


**Fig. 1** Flow chart of OA patients' enrollment and follow-up protocol. **A** Enrollment of OA patients and exclusion, dividing into two groups (HTO, HTO + AD-MSCs). **B** Timeline of treatment and clinical evaluation for the entire trial

injection, AD-MSC phenotype was assessed using flow cytometry. A cell suspension ($2\times10^6$ cells/ml) was prepared and mixed with mouse anti-human monoclonal antibodies to CD34 (catalog number 560942, BD, USA), CD44 (catalog number 555479, BD, USA), CD45 (catalog number 555483, BD, USA), CD73 (catalog number 561254, BD, USA), CD90 (catalog number 555596, BD, USA), CD105 (catalog number 560839, BD, USA), and HLA-DR (catalog number 560896, BD, USA). The mixture was incubated in a dark place for 20 min, washed, and the cells resuspended in 200 µl PBS. Phenotyping was then performed using the Guava easyCyte (MERCK Millipore, USA) flow cytometer. A microbiological safety examination was performed to identify the presence of

endotoxin, mycoplasmas (*Mycoplasma pneumoniae*, *Ureaplasma urealyticum*) and viruses (hepatitis B, hepatitis C, HIV, syphilis, and cytomegalovirus). Samples of AD-MSCs from each patient in passage 0 were stored in liquid nitrogen for future assay.

After passing the above tests, AD-MSCs were prepared as needed for intra-articular injection. The injection volume and number of cells were determined refer to published studies [32, 33]. For each patient, $5\times10^7$ cells were resuspended in injectable sterile isotonic (0.9%) normal saline to a total of 3 ml before injection. All injections were performed by a single surgeon at 1 month after HTO.

#### Clinical outcome measures

All data collection, measurements, and analyses were conducted by the same group of investigators who were blinded to the identity of each subject's experimental group. Clinical assessments included arthroscopic, radiological, and functional evaluations. Knee arthroscopy is the most reliable and precise method for assessing/observing articular cartilage status. The International Cartilage Repair Society (ICRS) grading system is a standardized method for assessing cartilage repair. It evaluates the quality and characteristics of cartilage tissue in both preclinical studies and clinical settings. Arthroscopic evaluation was carried out using the International Cartilage Repair Society (ICRS) classification system [34, 35]. Radiological evaluation was based on preoperative and 1-year postoperative knee MRI and X-ray images. MRI results were graded using a Modified MRI Grading System of the ICRS [36]. X-ray images were evaluated using the Kellgren–Lawrence (K–L) classification [37], Hip–Knee–Ankle (HKA) angle, and tibial plateau slope. At baseline, and at 6, 12, and 24 months postoperatively, all patients' Visual Analogue Scale (VAS) scores and Western Ontario and McMaster Universities Arthritis Index (WOMAC) scores [38] were evaluated to clinically assess changes in knee function. In terms of safety, postoperative complications were recorded, including complications such as nonunion of the osteotomy, infection, loosening of the internal fixation device, venous thromboembolism (VTE), and bone tumors.

#### AD-MSC resuscitation, culture, and passage

Based on the degree of cartilage repair observed arthroscopically for 24 months follow-up, we ranked and selected the top 5 (Sub-group **a**) and bottom 5 (Sub-group **b**) cases, based on ICRS scores, for further analysis stemness of the injected AD-MSCs. Sub-group a and sub-group b were chosen according to a multiple ranking system. The improvement in arthroscopic evaluation was considered to be the most important indicator, then MRI grading improvement, and WOMAC score. An aliquot of each patient's AD-MSCs that had been stored in liquid nitrogen immediately after isolation were thawed and then cultured in complete media containing MSCBM (catalog number 6114011, Dakewe, China), penicillin (100 U/ml), streptomycin (100 μg/ml) (catalog number P1400, Solarbio, China) and 5% serum substitute (UltroGRO, Helios, U.S.). Fifty percent media changes were performed every 3 days. For expansion, P1-P3 cells were seeded at $6\times10^3$ cells/cm$^2$ into 100 mm culture dishes and cultured for 7 days. For cell passage, incubation in 0.25% Trypsin–EDTA (catalog number 25200072, Gibco, USA) for 2 min was used and the number of cells counted using an automated cell counter (TC20, Bio-Rad, USA). Cell counting data were used to evaluate AD-MSC proliferation. The AD-MSC samples were used for further in vitro experiments (Supplemental Figure 1).

#### Colony forming unit (CFU) assays

For assay of CFU-fibroblasts (CFU-F), CFU-osteoblasts (CFU-OB) and CFU-adipocytes (CFU-AD), P1 and P3 cells were plated into six-well plates at 200 and 600 cells/well.

After 12 days of culture, CFU-AD samples were induced following the instructions accompanying an adipogenic differentiation kit (catalog number HUXMD-90031, Oricell, China) and culture for 7 days; similarly, CFU-OB samples were induced by following the instructions accompanying an osteogenic differentiation kit (catalog number HUXMD-90021, Oricell, China) and culture for 14 days. On day 14 of culture, samples for assay of CFU-F were fixed with 4% paraformaldehyde for 30 min, washed with 1×PBS, and stained with crystal violet (catalog number C0121, Beyotime, China) for 10 min to visualize the cell colonies. Analogously, after 14 days of incubation in osteoblast differentiation media, samples for assay of CFU-OB were fixed with 4% paraformaldehyde for 30 min, washed with 1×PBS, stained with Alizarin Red (catalog number ALIR-10001, Oricell, China) for 10 min, and then 1×PBS added to preserve cell morphology. Samples for assay of CFU-AD were fixed with 4% paraformaldehyde for 30 min, washed with 1×PBS, and then stained with Oil Red O (catalog number OILR-10001, Oricell, China) for 10 min.

#### Assay of beta-galactosidase (β-gal) activity and reactive oxygen species (ROS)

Staining for β-gal activity was used to assess the level of cellular senescence in the AD-MSC samples. P1 and P3 cells were seeded at $1.2\times10^4$ cells per well into 24-well

plates and cultured for 7 days. After fixation (catalog number C0602-1, Beyotime, China) for 15 min, cells were stained using a β-gal staining solution (catalog number C0602, Beyotime, China) at 37 °C overnight and then stored in 1×PBS at 4 °C.

To assess the level of ROS, P1 and P3 cells were seeded at $1.2\times10^4$ cells per well into 24-well plates, cultured for 7 days, and then assayed using a ROS assay kit (catalog number 50101ES01, Yeason, China), following the instructions accompanying the kit. The amount of ROS present was observed and documented using an inverted phase contrast fluorescence microscope.

#### Transmission electron microscopy (TEM)

Alterations of AD-MSCs function correlated with cellular structure, and TEM is a powerful technique that allows for the detailed visualization of cellular structures. We intended to compare sub-group a with sub-group b through TEM assay, which provided critical insights into the mechanisms. Cells were collected and fixed in TEM fixative (catalog number G1102 Servicebio, China), and in turn were subjected to agarose pre-embedding, post-fixation, dehydration, resin infiltration, polymerization, ultramicrotomy to prepare thin sections (Leica UC7 Leica, Germany), and staining. Finally, the cells were observed under TEM (HT7800, HITACHI, Japan) to prepare transmission electron micrographs.

#### Transcriptome with genome and bioinformatic analysis

Transcriptome with genome technology is provided by Nanjing Genepioneer Biotechnologies. All RNA samples of human AD-MSCs from sub-group a and sub-group b were collected and library preparations for transcriptome sequencing were completed and sequenced. Raw data were processed to obtain clean data and all downstream analyses were based on clean data with high quality. Reference genome and gene model annotation files were downloaded from genome website directly. Index of the reference genome was built and paired-end clean reads were aligned to the reference genome using HISAT2. StringTie was used to count the reads numbers mapped to each gene and FPKM was calculated. Differential expression analysis of two conditions/groups was performed using the DESeq2 R package (1.26.0). FDR < 0.05 and $|\text{Log2(Fold change)}| \geq 1$ was set as the threshold for significantly differential expression. Gene function was annotated based on the following databases: Nr (NCBI non-redundant protein sequences); Nt (NCBI non-redundant nucleotide sequences); Pfam (Protein family); KOG/COG (Clusters of Orthologous Groups of proteins); Swiss-Prot (A manually annotated and reviewed protein sequence database); KO (KEGG Ortholog database); GO (Gene Ontology).

#### Statistical analysis

In this study, quantitative data such as age and weight were analyzed using mean ± standard deviation (X ± SD). Clinical data, including VAS and WOMAC scores, activity level, and angles were evaluated based on their distribution. A t-test was used for comparison if the data followed a normal distribution, otherwise, a non-parametric test was applied. For between-group comparison of cartilage grade and K–L classification, the Mann–Whitney U rank-sum test was used. All statistical analyses were conducted using SPSS version 26.0 (SPSS, USA). *P*-values < 0.05 were considered statistically significant.

## Results

#### The baseline demographic characteristics of the control (HTO) and experimental (HTO + AD-MSCs) subjects were similar

After screening all potential study participants, a total of 45 subjects were ultimately enrolled in the study (Fig. 1). Group 1 controls (HTO only) consisted of 22 patients, while Group 2 experimentals (HTO + AD-MSCs) consisted of 23 patients. As can be seen in Table 1, there are no statistically significant differences between the two groups of participants in terms of baseline characteristics, including gender, age, knee with OA (left/right), weight, height, body mass index (BMI), length of follow up, and Kellgren–Lawrence (K–L) grade.

Perioperative clinical and radiological data for the control and experimental groups showed no significant differences (Table 2), including duration of the HTO operation, osteotomy opening angle and height, length of post-operative hospital stay, pre-operative and post-operative hip–knee–ankle (HKA) angle, and tibial plateau slope. In terms of safety and complications, neither group experienced a non-union of the osteotomy, infection,

**Table 1** Baseline demographic characteristics of study participants

| | HTO (n = 22) | HTO + AD-MSCs (n = 23) | *p* |
|---|---|---|---|
| Gender (M/F) | 9/13 | 9/14 | 0.91 |
| Age (yrs) | 54.55 ± 7.18 | 54.57 ± 7.79 | 0.99 |
| OA side (L/R) | 10/12 | 11/12 | 0.87 |
| Body weight (kg) | 75.57 ± 13.67 | 71.70 ± 11.80 | 0.31 |
| Height (cm) | 166.37 ± 5.73 | 164.84 ± 7.89 | 0.46 |
| BMI (kg/m$^2$) | 26.5 ± 2.3 | 26.7 ± 2.5 | 0.79 |
| Follow up (months) | 32.00 ± 4.92 | 30.64 ± 5.06 | 0.37 |
| K–L Grade (I/II/III) | 7/11/4 | 6/9/8 | 0.45 |

**Table 2** Perioperative clinical and radiological data for control and experimental subjects

| | HTO | HTO + AD-MSCs | P value |
|---|---|---|---|
| HTO duration (min) | 107.50 ± 31.24 | 118.04 ± 38.40 | 0.32 |
| Opening angle (°) | 11.20 ± 4.47 | 10.62 ± 3.72 | 0.64 |
| Opening height (mm) | 13.13 ± 5.01 | 12.42 ± 4.82 | 0.63 |
| Postoperative hospital stay (days) | 5.73 ± 1.32 | 5.91 ± 1.28 | 0.65 |
| HKA (°) | | | |
| Pre-OP | 171.00 ± 4.83 | 171.67 ± 2.34 | 0.55 |
| Post-OP | 180.95 ± 3.13 | 181.37 ± 3.12 | 0.65 |
| Tibial plateau slope (°) | | | |
| Pre-OP | 10.44 ± 2.48 | 10.78 ± 2.47 | 0.65 |
| Post-OP | 10.89 ± 3.41 | 9.05 ± 3.23 | 0.07 |

implant loosening, venous thromboembolism (VTE), or other serious complications during the follow-up.

### Cartilage repair and regeneration were promoted by the injection of AD-MSCs after HTO surgery

MRI and arthroscopy were used to evaluate articular cartilage status before surgery and 12 months after HTO alone or HTO followed by intra-articular injection of AD-MSCs (Fig. 2). Prior to treatment, MRI images (upper panel) show the presence of knee inflammation (yellow arrows indicate edema) and loss of articular cartilage (red arrows), while 12 months after HTO and injection of AD-MSCs the same articular surface is smooth with no signs of inflammation. These representative case of MRI images were chosen by the median of patients arranged by grade. Arthroscopy of the joint (lower panels) confirmed the MRI observations and showed condyle cartilage injury and a clear view of the vascularized underlying bone before the operation and a repaired lesion showing newly formed white cartilage at 12 months after HTO and injection of AD-MSCs.

Based on the encouraging imaging studies, we proceeded to quantitate cartilage repair using the International Cartilage Repair Society (ICRS) grading system (Fig. 2B, C). At baseline, there was no statistical difference in ICRS grades (using the MRI and arthroscopy images) between the two groups of subjects. After HTO alone, the 1-year postoperative ICRS grading of the MRI results showed that the number of patients in each grade was distributed as follows: Grade I: 4 (18%), Grade II: 4 (18%), Grade III: 5 (23%), and Grade IV: 9 (41%). In contrast, after HTO followed by injection of AD-MSCs, the number of patients in each grade was distributed as follows: Grade I: 10 (43%), Grade II: 6 (26%), Grade III: 3 (13%), and Grade IV: 4 (17%), suggesting that the combination of both surgery and stem cells significantly reduced the severity of OA as compared to patients treated with HTO alone. Next, we validated the results using arthroscopic images which allowed direct observation of the knee articular cartilage. Consistent with the MRI results, the arthroscopy showed that the number of patients in each grade after HTO alone was as follows: Grade I: 4 (18%), Grade II: 7 (31%), Grade III: 6 (27%), and Grade IV: 5 (23%). In contrast, after HTO followed by injection of AD-MSCs, the number of patients in each grade were distributed as follows: Grade I: 10 (43%), Grade II: 9 (39%), Grade III: 3 (13%) and Grade IV: 1 (4.3%). These data are graphically displayed in Fig. 2B, C and show that the proportion of patients with severe knee OA was significantly reduced after the combined treatment (HTO + AD-MSCs) versus HTO alone.

To evaluate improvement in functionality and pain relief, WOMAC and VAS assessments were performed at 0, 6, 12, and 24 months after treatment (Fig. 2D, E). The results showed that there was no improvement in the VAS assessment; however, by 24 months there was a statistically significant reduction in WOMAC scores for the HTO + AD-MSC versus HTO group.

### Stemness and senescence of the injected AD-MSCs determine therapeutic effect

#### *Based on arthroscopic findings (ICRS grades I–IV), the top 5 and bottom 5 patients were selected for a comprehensive analysis of AD-MSC phenotype*

Since there was such a wide variation in arthroscopic findings, no statistically significant differences could be discerned when all of the ICRS scores (i.e. grades) were averaged and then compared (HTO versus HTO + AD-MSC groups). To test whether the observed differences were correlated with variability in stemness of autologous of AD-MSCs, we chose the top 5 patients with an ICRS Grade of I as a sub-group "**a**" and the bottom 5 patients with an ICRS grade of III–IV as a sub-group "**b**" from the HTO + AD-MSCs group for comprehensive analysis of their AD-MSCs.

The individual improvement of ICRS grades for patients in sub-groups **a** and **b** were statistically different (Fig. 3A); in contrast, patients in sub-group **b** were not different from those in the HTO group, while patients in sub-group **a** were significantly different. Overall, patients in sub-groups **a** and **b** were not statistically different regarding age or BMI (Fig. 3B, C). To exclude the influence of surgical factors, we compared the major indicator, postoperative HKA angle, between the two subgroups. Results showed that the lower limb alignment after HTO were basically consistent (Fig. 3D). As a part of our quality control process, we routinely analyze MSCs for the expression of specific sets of surface markers before administration to

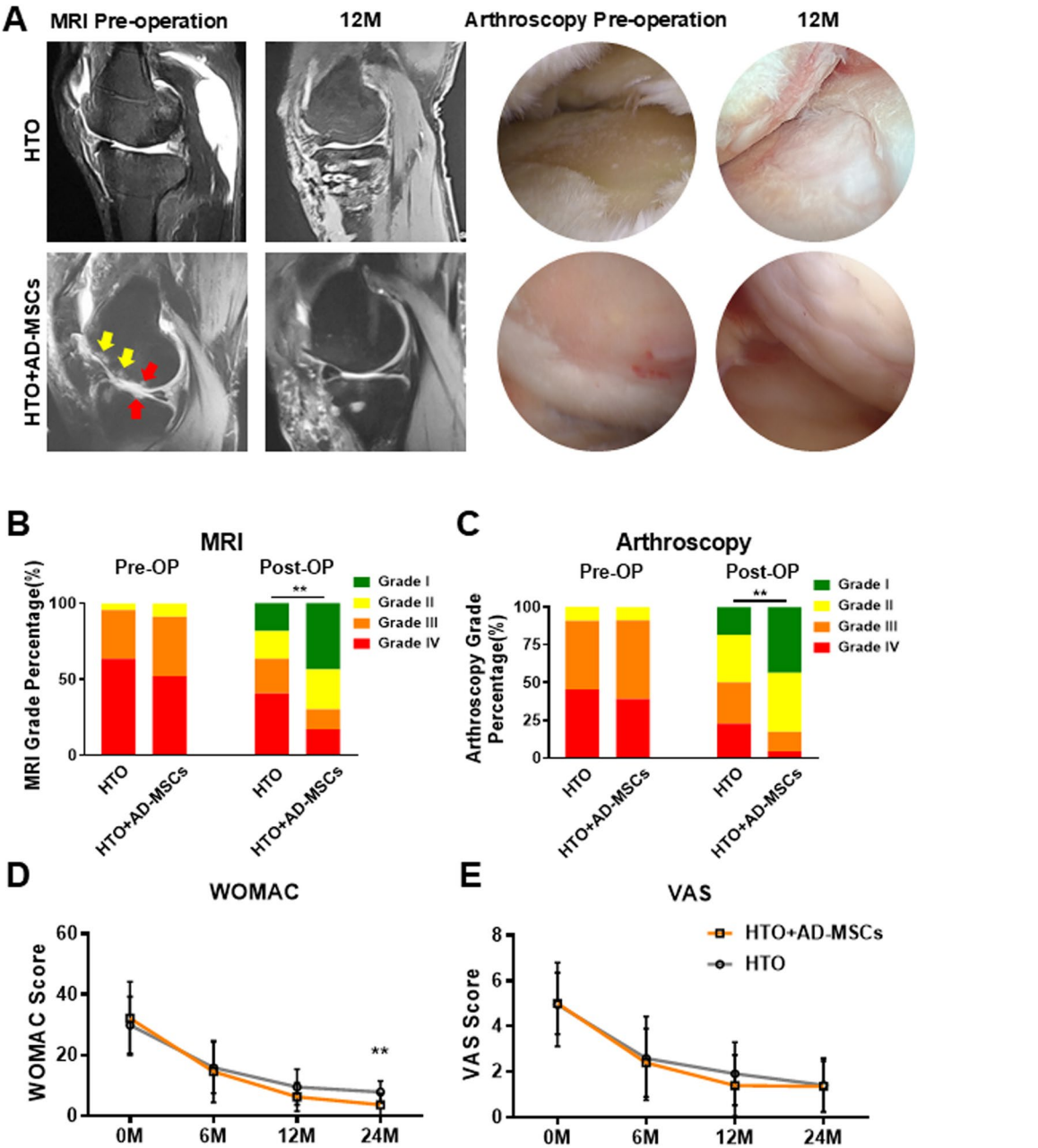


**Fig. 2** Clinical evaluation of the HTO and HTO + AD-MSCs groups. **A** Representative MRI (sagittal axis) images from same patient, comparing the preoperative (HTO: Grade III; HTO + AD-MSCs: Grade IV) and 12 months post treatment (HTO: Grade III; HTO + AD-MSCs: Grade II). Representative arthroscopy images from same patient, comparing the preoperative (HTO: Grade III; HTO + AD-MSCs: Grade IV) and 12 months post treatment (HTO: Grade II; HTO + AD-MSCs: Grade I). **B**, **C** International Cartilage Repair Society (ICRS) grading of pre-operative and post-operative (12 month) MRI and arthroscopy images of a representative knee joint from subjects in the HTO and HTO + AD-MSCs groups. **P < 0.05, HTO versus HTO + AD-MSC groups at 12 months post-op. **D** Western Ontario and McMaster Universities Arthritis Index (WOMAC) scores at 0, 6, 12, 24 months (M) after treatment (post-op) between HTO and HTO + AD-MSCs groups. **P < 0.05 (n = 5), HTO versus HTO + AD-MSC groups at 24 months. **E** Visual Analogue Scale (VAS) scores at 0, 6, 12, 24 months (M) after treatment (post-op) between HTO and HTO + AD-MSCs groups. No significant differences were noted

the patients, as prescribed by the International Society for Cellular Therapy position statement (ISCT) [39]. In our analysis of sub-group **a** and **b**, we found that > 95% of the cells consistently expressed CD90, CD105, CD73 as well as CD44 with no significant differences between the two groups (Fig. 3E–H). In addition, < 1%

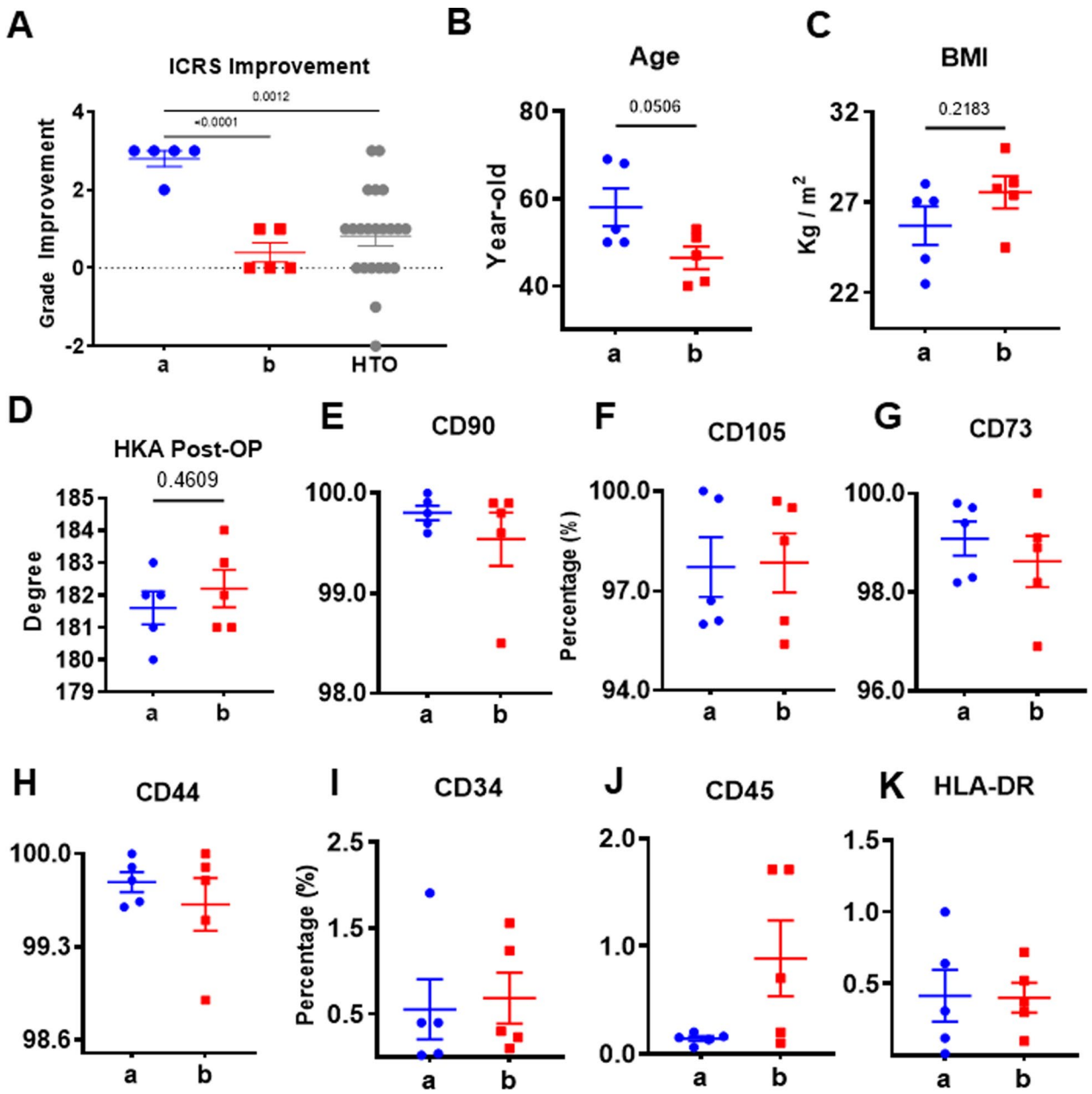


**Fig. 3** Comparison of sub-groups **a** and **b** based on ICRS grade, patient age and BMI, and MSC surface marker expression. **A** ICRS grades improvement of the top 5 (**a**) and bottom 5 (**b**) patients in the HTO + AD-MSC group compared to HTO alone. There was a statistically significant difference between sub-groups **a** and **b** and group **a** and HTO. Mean ± SD, **P < 0.05 (n = 5), vs. the indicated group. **B**, **C** Age and BMI were comparable between sub-group **a** and sub-group **b**. **D** Postoperative HKA angle, between sub-group **a** and sub-group **b**. **E**–**K** Percent cell surface marker expression using FACS analysis

of AD-MSCs from both sub-groups expressed CD34, CD45 and HLA-DR (Fig. 3I–K). Taken together, these data suggest that the AD-MSCs from both sub-groups were very similar in terms of their surface marker expression profiles.

***AD-MSCs from patients with the most improvement (lower ICRS scores) had higher proliferation rates and produced more numbers of CFUs than those from patients showing less improvement (higher ICRS scores)***

To determine whether the wide variation in clinical outcomes was related to the stemness of the injected AD-MSCs, we studied the proliferation of each subject's

AD-MSCs by subculturing their cells for 3 passages (7 days/passage). The cell counts for both sub-groups dropped with increasing number of passages (Fig. 4A), but cells in sub-group **a** proliferated to a significantly greater extent than those in sub-group **b** at all three passages. Cell doubling time in sub-group **a** was significantly shorter and relatively stable as compared to that of sub-group **b** (Fig. 4B). These results suggest that the proliferation capacity of sub-group **a** cells was superior to that of sub-group **b** cells.

Next, the number of colony forming cells produced by AD-MSCs in sub-groups **a** and **b** were compared using colony forming unit (CFU) assays for Fibroblasts (CFU-F), Osteoblasts (CFU-OB), and Adipocytes (CFU-AD). MSCs from sub-group **a** formed a greater number of CFU-F, (twofold greater at passage 1 [P1]), which were larger and more densely stained, than those from sub-group **b** (Fig. 4C, D). We also compared the ability of AD-MSCs from sub-groups **a** versus **b** to differentiate into osteoblasts (CFU-OB) or adipocytes (CFU-AD) in response to each lineage's differentiation media. The degree of Alizarin Red staining for mineral in each CFU-OB, as well as the number of CFU-OB at P1 and P3, was higher from cells in sub-group **a** than sub-group **b** (Fig. 4C, D). Moreover, we found more Oil red O-stained adipocytes in each CFU-AD with higher numbers of CFU-AD formed by AD-MSCs (P1 and P3) from sub-group **a** than sub-group **b** (Fig. 4C, D). Microscopic observations of CFU-F, CFU-OB, and CFU-AD were showed in Supplemental Figure 2.

#### *AD-MSCs from sub-group "a" contained fewer senescent cells and generated less reactive oxygen species (ROS) than AD-MSCs from sub-group "b"*

To further compare the quality of AD-MSCs in the two sub-groups, we measured cellular senescence by assaying β-galactosidase (β-gal) activity and intracellular ROS levels. The data revealed the presence of more β-gal positive cells, as well as increased levels of ROS, in AD-MSCs from sub-group **b** than in sub-group **a** (Fig. 5A, B).

Since mitochondria are involved in ROS generation [40], we examined the ultrastructure of mitochondria using transmission electron microscopy (TEM). Cells from sub-group **b** showed more signs of mitochondrial damage (yellow arrows), such as internal disintegration, swelling, and rupture of the cristae, than cells from sub-group **a** (Fig. 5C). In sub-group **a**, the number of normal mitochondria per cell was significantly larger than sub-group **b** (Fig. 5D). This suggests that mitochondrial damage and elevated ROS levels may influence stem cell senescence, which ultimately determines the clinical outcome of intra-articular stem cell injections.

#### *Analyzing differences between AD-MSCs from sub-group "a" and "b" by RNA-sequencing*

10 samples were collected, including 5 in sub-group "**a**" and 5 in sub-group "**b**", and RNA-sequencing were performed, which may provide a deeper view in AD-MSCs regulation. First, Principal Component Analysis (PCA) was performed to deeply explore the relationships between these samples and the magnitude of variation. The results indicated that AD-MSCs from sub-group a and b were different, though all were AD-MSCs from adipose tissue (Fig. 6A). Then, differential gene expression analysis was conducted. We have detected that there are indeed some differences between sub-group "**a**" and sub-group "**b**", however, molecule and signaling pathway changes are the most important. In total, 304 genes with significantly different expression were identified, consisting of 66 genes upregulated and 238 genes downregulated, in which sub-group **a** was as control (Fig. 6B, C). There are individual differences in each group, considering the individual differences are inevitable. After further analysis of different expression genes by KEGG enrichment analysis and GO enrichment analysis (Fig. 6D–G), we found that genes related with cellular processes especially cell growth and death were enriched such as CCNB1, CCNB2, CDK1 and CDC20. Specifically, differentially expressed genes were enriched in cell cycle, mitotic process and cellular senescence. Further, as most enrichment analysis demonstrated the pivotal role of cell cycle pathway, we performed GSEA to explore the expression details and alterations in sub-group **a** and **b**. Genes related with cell cycle pathway were mostly located in sub-group **a**, revealing the essential role of cell cycle in AD-MSCs (Fig. 6H). Taken together, cell cycle

(See figure on next page.)

**Fig. 4** Assay of AD-MSC proliferation and comparison of CFUs generated by AD-MSCs from sub-groups **a** and **b**. **A** Cell number (mean ± SD) was determined at the end of each passage (P1, P2, and P3) and presented as cell number/cm$^2$. Cells from both sub-groups were plated using the same seeding density (6000 cells/cm$^2$) and sub-cultured for 3 passages (7 days/passage). **B** Cell doubling time (mean ± SD) was calculated at the end of each passage. **P < 0.05 (n = 5), vs. sub-group b at the same passage. **C** Images of CFU-F, CFU-OB and CFU-AD formed by P1 and P3 AD-MSCs; 5 patients (numbers of 1–5) from sub-group **a** (ICRS score of I) and group **b** (ICRS score of III–IV) were analyzed to perform the comparison. All CFU assays for each patient were performed in triplicate. **D** Numbers of CFU-F, CFU-OB, and CFU-AD per well were performed in triplicate for each patient. The data shown consist of 15 values (3/patient with 5 patients/sub-group). **P < 0.05 (n = 15) vs. sub-group **b** based on mean ± SD at the same passage

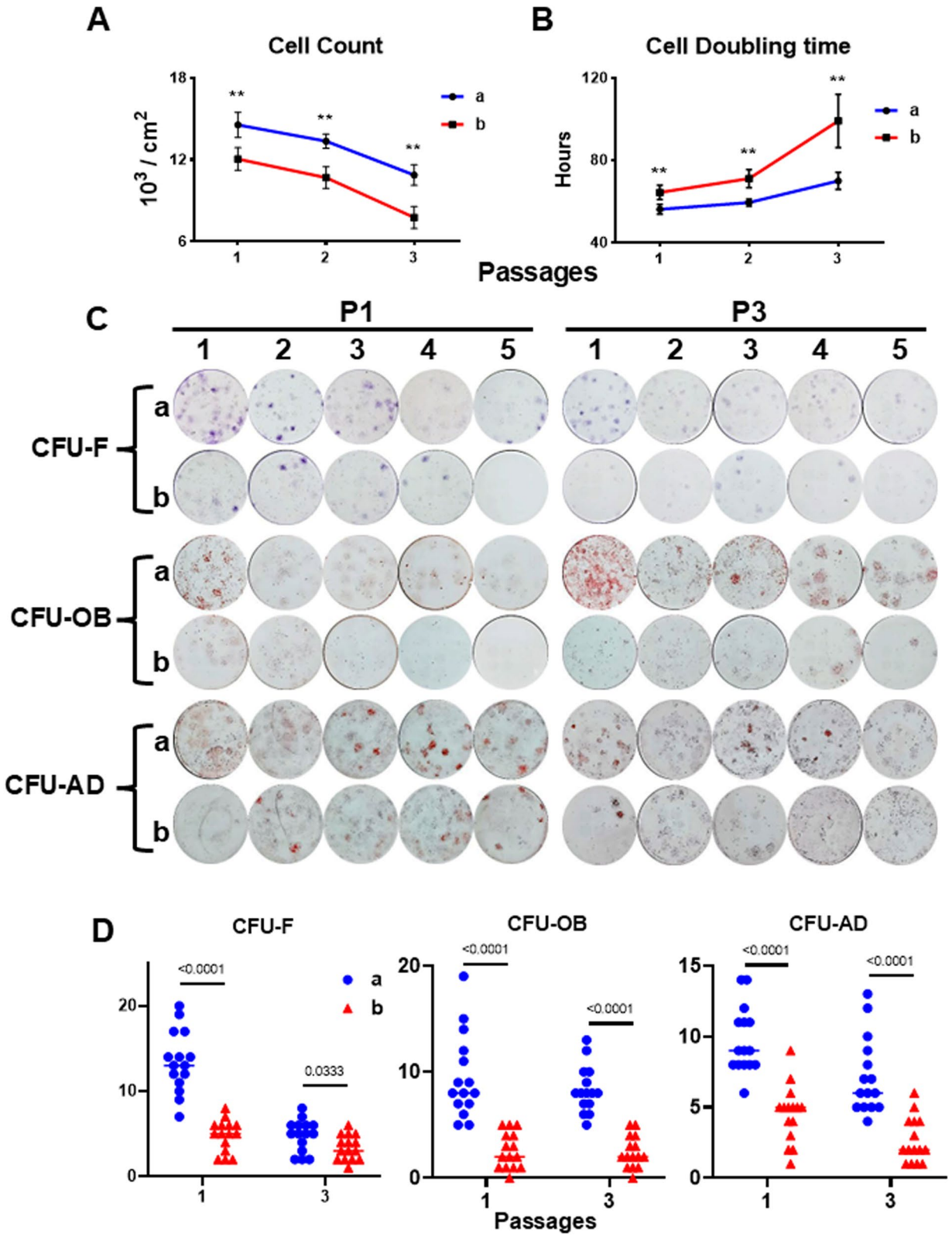


**Fig. 4** (See legend on previous page.)

pathway might correlate with the regeneration and repair capacity of ADMSCs and more exploration was needed in the future. These results revealed that genes connected with cell cycle were the possibly regulatory targets to prevent cell senescence and therapeutic effect of AD-MSCs.

## Discussion

During the last two decades, approximately 25 studies, which include ~500 knee OA patients treated with MSCs, have been fully described; notably, about 80% (20 out of 25) of these studies were conducted with patients who received autologous MSCs [12]. In the 20 studies investigating autologous stem cell therapy, 6 studies utilized autologous bone marrow-derived mesenchymal stem cells (BM-MSCs), 13 studies used autologous adipose-derived mesenchymal stem cells (AD-MSCs), and 1 studies employed autologous activated peripheral blood stem cells (AAPBSCs). Among the 6 studies using autologous BM-MSCs, 4 were randomized controlled trials (RCTs) and 2 were non-randomized comparative studies [14, 41–45]. Notably, only one (16.7%) of these studies reported satisfactory therapeutic outcomes. Of the 13 studies utilizing autologous AD-MSCs, 4 were RCTs and 9 were non-randomized comparative studies [15, 33, 46–53]. Among these, 6 (46.2%) studies demonstrated satisfactory therapeutic effects. The single study investigating autologous activated peripheral blood stem cells reported only fair outcomes [54]. It is important to note that some of these studies administered stem cell injections alone, while others combined them with additional biological agents. Moreover, the control group interventions varied across these studies, contributing to the heterogeneity of the results.

These variations in study design, MSC source, treatment protocols, and control interventions may partly explain the inconsistency in reported outcomes across studies. This underscores the need for more standardized protocols to accurately assess the efficacy of MSC-based therapies for OA. Overall, the clinical outcomes of these studies show a large variation in improvement between MSC and control groups. Here, we provide strong evidence demonstrating that there is substantial biological variability in the function of autologous AD-MSCs and this variability likely contributes to the inconsistent clinical outcomes reported.

HTO is a surgical procedure used to realign the load-bearing axis of the knee and relieve pain, retard articular cartilage degeneration, and postpone the need for a total knee arthroplasty [55, 56]. However, HTO alone has limited capacity to repair cartilage damage, resulting in short term improvement [57, 58]. Others have previously reported that HTO combined with intra-articular injection of MSCs repairs articular cartilage lesions and improves knee function better than HTO alone [15, 42]. In the current study, we showed that HTO + AD-MSCs significantly reduced the severity of knee OA, as compared to HTO alone, based on MRI and arthroscopic findings. These results support the previous obtained observations.

In the present study we tested, for the first time, the hypothesis that the wide variation in clinical outcomes, previously reported by others, is correlated with the biological variability of each patient's own (i.e., autologous) MSCs. To test our hypothesis, we stored an aliquot of each patient's AD-MSCs in liquid nitrogen for future cell studies. We compared the quality of the archived AD-MSCs obtained from patients in the HTO + AD-MSC group: 5 patients showing the most improvement based on ICRS score (sub-group **a**) and 5 patients showing the least improvement based on ICRS score (sub-group **b**). Remarkably, proliferation and CFU-F efficiency of all 5 patients in sub-group **a** were significantly higher than those from the 5 patients in sub-group **b** during multiple passages and sub-culture (Fig. 4). Since not all the CFU-F are able to differentiate into osteoblasts or adipocytes, the differentiation capacity of the CFU-Fs to CFU-OB and CFU-AD was determined by treatment with osteoblast or adipocyte differentiation media, respectively. The results showed that the majority of CFU-Fs generated by AD-MSCs from patients in sub-group **a** were able to differentiate into CFU-OB and CFU-AD, many of which were higher than those formed by AD-MSCs from patients in sub-group **b** (Fig. 4). Moreover, the increased

(See figure on next page.)

**Fig. 5** Comparison of senescent cells and intracellular ROS levels and transmission electron micrographs of AD-MSCs from sub-groups **a** versus **b**. Passage 1 and 3 AD-MSCs were seeded onto tissue culture plastic (TCP) at 6000 cells/cm$^2$ and cultured for 7 days (> 80% confluent). Senescent cells were detected by β-galactosidase (β-gal) staining, while intracellular ROS levels were measured using 2′,7′-dichlorofluorescin diacetate (DCFHDA). **A** Images obtained from 5 individual patients (numbers of 1–5) for each sub-group. Upper panel: β-gal positive cells (brightfield microscopy); and lower panel: ROS positive cells (fluorescence microscopy). **B** Numbers of positive cells were counted (each of the 5 donor's cells [per sub-group] was assayed in triplicate), the data presented by sub-group, and statistical comparisons performed. **P < 0.05 (n = 15), vs. sub-group **b** (mean ± SD) at the same passage. **C** Mitochondrial ultrastructure is shown in a high magnification version (lower panel, "40X") of the low magnification version (upper panel, "10X"). Yellow arrows indicate mitochondrial damage (enlarged or dense cored vesicles). **D** The number of normal mitochondria per cell

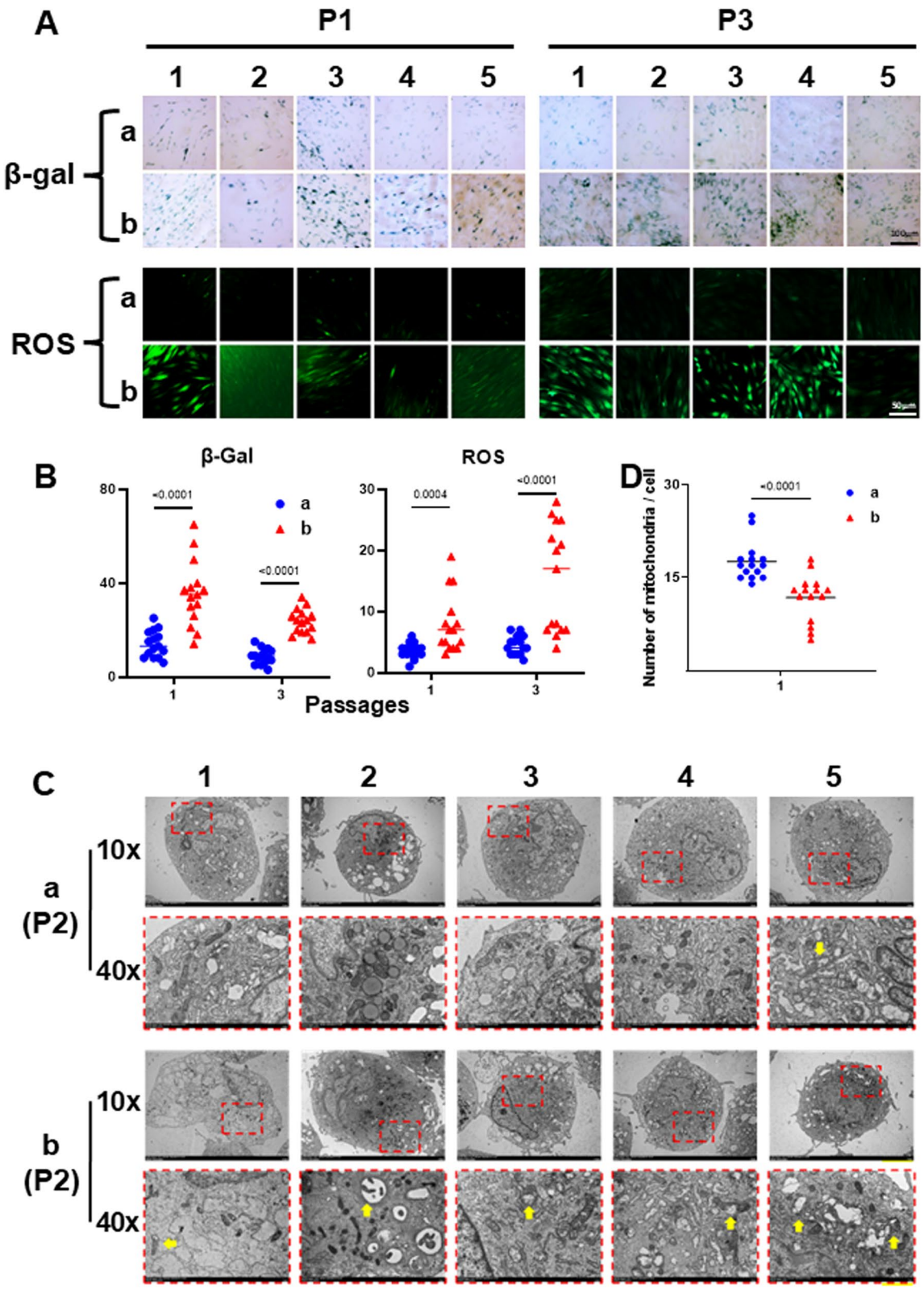


**Fig. 5** (See legend on previous page.)

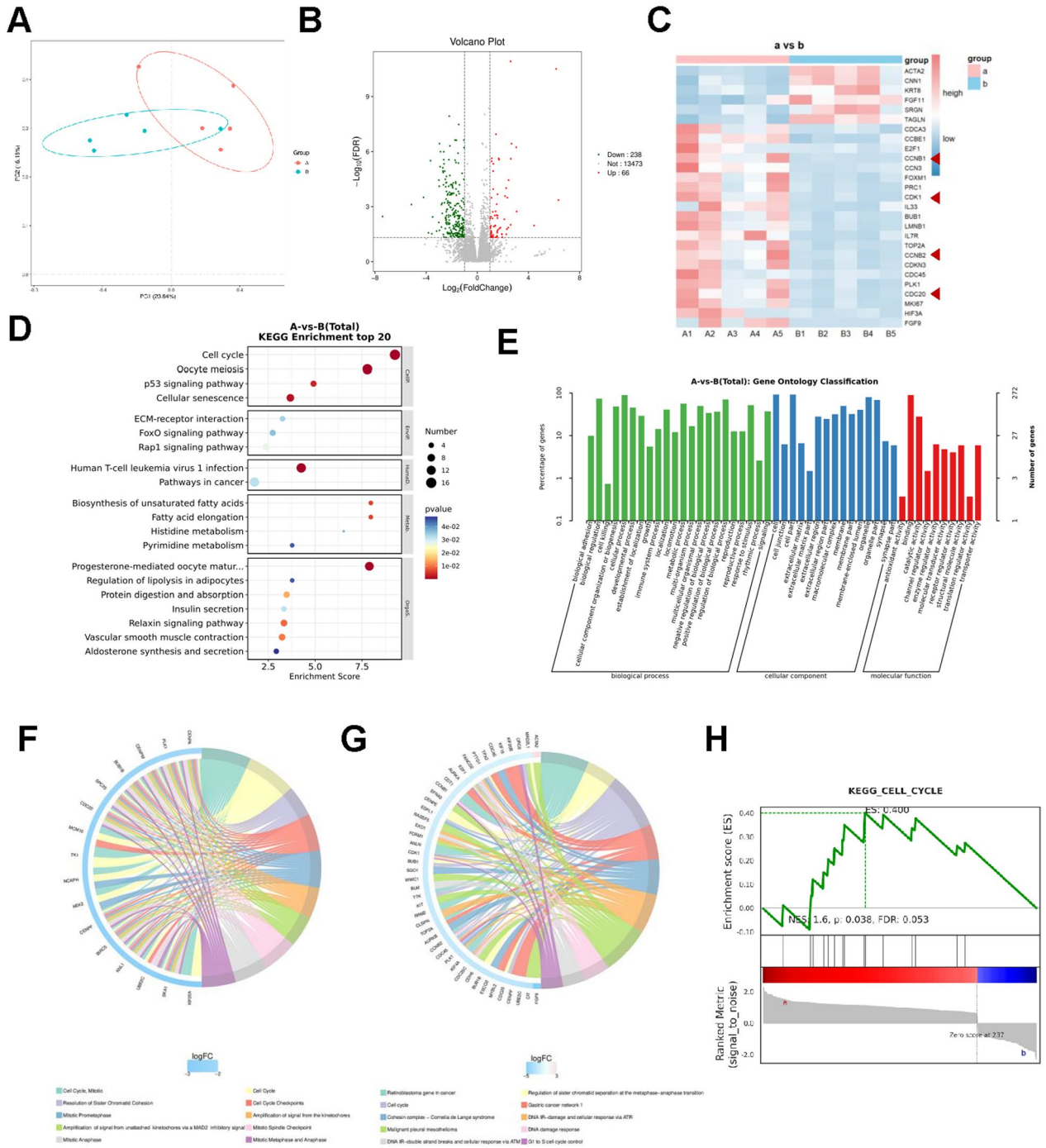


**Fig. 6** RNA-sequencing of AD-MSCs from sub-groups **a** and **b**. **A** Principal Component Analysis (PCA) plot showing the distribution of samples from sub-group **a** and **b** along the first two principal components (PC1 and PC2). The percentages on the axes represent the proportion of total variance explained by PC1 and PC2. **B** Volcano Plot of 10 individuals' AD-MSCs from sub-groups **a** and **b**. |Log2(Fold change)| ≥ 1, FDR < 0.05, 238 genes (green plots) were down-regulated and 66 genes (red plots) were up-regulated ( sub-group **a** as control). **C** Clustering heat map of 10 individuals' AD-MSCs from sub-groups **a** and **b** (red arrows showed CCNB1, CCNB2, CDK1, and CDC20). **D**–**G** GO and KEGG enrichment analysis of different expression genes. **H** Gene Set Enrichment Analysis (GSEA) results illustrating the cell cycle pathway gene sets in sub-group **a** and **b**. ES (enrichment score), p-value and FDR were shown

amount of proliferation and ability to form CFUs shown by sub-group **a** cells might be due to the low level of ROS production and senescent cells present compared to sub-group **b** cells (Fig. 5). It was also evident that lower amounts of ROS production was associated with the presence of more intact mitochondria in AD-MSCs from the patients showing more improvement in OA symptoms (Fig. 5). Taken together, these results suggest that clinical outcomes are strongly correlated with the stemness and senescence of the autologous AD-MSCs injected into the joint; cell qualities such as the capacity for proliferation, colony formation (reflecting CFU efficiency), and differentiation, and the effects of aging on MSCs (e.g. cellular senescence and intracellular ROS production). The present studies also suggest that although these cell qualities may have the potential to predict clinical outcome, MSC surface markers (e.g. CD90, CD105, and CD73), as recommended by the ISCT for routinely assessing MSC quality, did not demonstrate any potential for predicting efficacy.

A review of the published reports describing the results of MSC-based clinical trials for knee OA, ~80% employed autologous MSCs due to biosafety concerns and increasing evidence suggesting that MSCs may not be immune privileged [17]. Our study also indicated that the senescence level of AD-MSCs had a crucial impact on the therapeutic effect. In addition, senescent cells increase with aging and acquire a senescence-associated secretory phenotype (SASP) which is characterized by the release of cytokines, chemokines, growth factors, and proteases, which impair adjacent MSCs and contribute to aging-associated degenerative pathologies [59, 60]. Furthermore, it has been confirmed that oxidative stress in aging caused by dysregulated accumulation of ROS may induce cellular senescence of human MSCs and further affect stem cell function [61, 62]. Since elderly patients are the primary target population for cell-based treatment of age-related diseases such as knee OA, the quality of autologous MSCs are compromised due to aging and further influenced by other diseases (e.g. diabetes, heart disease) and multiple medicines. In particular, patients with autoimmune diseases often take steroids (e.g. glucocorticoids drugs) that can induce apoptosis of MSCs [63, 64]. Interestingly it has been reported that old-MSCs can be rejuvenated by exposure to a young microenvironment [65, 66]. By combining the findings reported in the current study, where the quality of an individual's own MSCs (autologous MSC therapy) can be predicted with some success, with the ability to rejuvenate MSCs from elderly donors by culture on a young microenvironment, it's possible that in the future we may be able to predict the likelihood of clinical success using one's own cells.

There were some limitations in this study. Although we believe that preserving the multiple samples of AD-MSCs from the same individual as the injected cells is already valuable. Cell samples used for in vitro experiments were not from the same culture batch as the injected cells, because the time of individual enrollment is dispersed over years. When conditions permit, direct comparison of the injected cells is preferable. Moreover, large sample size, long-term follow-up studies with further mechanism discussion are still needed in the future to help better understand the safety and therapeutic potential of AD-MSCs.

In summary, our findings strongly support the hypothesis that the inconsistent clinical outcomes of autologous MSC-based therapy are correlated with the variability of the stemness and senescence of the injected MSCs. More importantly, the results indicate that the properties of MSC proliferation and differentiation, CFU efficiency and cell senescence and ROS could be used as sets of criteria to predict the clinical outcomes for autologous MSC-based therapy for knee OA. To improve the clinical efficacy, we propose to rejuvenate autologous MSCs by exposure to a young microenvironment to standardize the stemness and senescence of autologous MSCs prior to the administration. Finally, our study highlights emerging opportunities and trends in precision medicine that could potentially improve autologous MSC-based therapies.

## Conclusions

Clinical outcomes of autologous AD-MSCs therapy in knee osteoarthritis are correlated with stem cell stemness and senescence. The analysis of autologous stem cells may provide a reference for patient selection and efficacy prediction for osteoarthritis, and inspire new strategies for cell pretreatment. Our study highlights emerging opportunities and trends in precision medicine that could potentially improve autologous MSC-based therapies.

## Supplementary Information

The online version contains supplementary material available at https://doi.org/10.1186/s12967-024-05814-3.

Supplementary Material 1.

**Acknowledgements**
Not applicable.

**Author contributions**
PL and HS participated in conception and design, collected and analyzed the patient data regarding the clinical symptoms and examination. HZ, KH, HM, YT performed and analyzed the cell experiment of AD-MSCs. QL, LC, SL and ZL analyzed the clinical and experiment data in this study. HS and HZ wrote the manuscript. LZ and PL participated in conception and design, reviewed the

manuscript, and gave final approval for manuscript submission. All authors read and approved the final manuscript.

**Funding**
This work was supported by grants from the National Natural Science Foundation of China (82302699, 82472424), and China Postdoctoral Science Foundation (2023M732099).

**Availability of data and materials**
The datasets used and/or analyzed during the current study are available from the corresponding author on reasonable request.

## Declarations

**Ethics approval and consent to participate**
This clinical study was a prospective, randomized, open-label, blind end point trial conducted at a single institution. The project was approved by the Ethics Committee of Qilu Hospital of Shandong University (approval number: 2018-023) with the title "Effectiveness of Autologous Adipose-derived Stem Cells in the Treatment of Knee Cartilage Injury" on August 1st, 2018. The study was registered on the U.S. National Institutes of Health sponsored website, www.ClinicalTrials.gov, under the identification number, NCT03955497, before any subjects were enrolled. Informed consent was obtained from all the subjects prior to active participation in the study.

**Consent for publication**
Informed consent was obtained from all the subjects prior to active participation in the study.

**Competing interests**
The authors declare that they have no competing interests.

**Author details**
[1]Department of Orthopedics, Qilu Hospital of Shandong University, Cheeloo College of Medicine, Shandong University, Jinan 250012, China. [2]Qilu Cell Therapy Technology Co., Ltd, Jinan, China. [3]Key Laboratory of Chemical Biology (Ministry of Education), School of Pharmaceutical Sciences, Cheeloo College of Medicine, Shandong University, Jinan, China. [4]Department of Joint Surgery, Weifang People's Hospital, Weifang 261000, Shandong, People's Republic of China.

Received: 19 June 2024 Accepted: 29 October 2024
Published online: 18 November 2024

**References**

1. Ehioghae M, Vippa TK, Askins D, Slusarczyk S, Bobo E, Montoya A, Anderson D, Robinson CL, Kaye AD, Urits I. Exploring orthopedic stem-cell approaches for osteoarthritis management: current trends and future horizons. Curr Pain Headache Rep. 2024;28(1):27–35.
2. Sharma L. Osteoarthritis of the knee. N Engl J Med. 2021;384(1):51–9.
3. Smith HS. Potential analgesic mechanisms of acetaminophen. Pain Physician. 2009;12(1):269–80.
4. Ghanem CI, Pérez MJ, Manautou JE, Mottino AD. Acetaminophen from liver to brain: new insights into drug pharmacological action and toxicity. Pharmacol Res. 2016;109:119–31.
5. Ekhtiari S, Haldane CE, de Sa D, Simunovic N, Musahl V, Ayeni OR. Return to work and sport following high tibial osteotomy: a systematic review. J Bone Joint Surg. 2016;98(18):1568–77.
6. Katz JN, Arant KR, Loeser RF. Diagnosis and treatment of hip and knee osteoarthritis: a review. JAMA. 2021;325(6):568–78.
7. Karsdal MA, Bay-Jensen AC, Lories RJ, Abramson S, Spector T, Pastoureau P, Christiansen C, Attur M, Henriksen K, Goldring SR, Kraus V. The coupling of bone and cartilage turnover in osteoarthritis: opportunities for bone antiresorptives and anabolics as potential treatments? Ann Rheum Dis. 2014;73(2):336–48.
8. Yu H, Huang Y, Yang L. Research progress in the use of mesenchymal stem cells and their derived exosomes in the treatment of osteoarthritis. Ageing Res Rev. 2022;80: 101684.
9. Matsuta S, Endo K, Ozeki N, Nakagawa Y, Koga H, Sekiya I. Synovial mesenchymal stem cells secrete more lubricin than adipose mesenchymal stem cells after injection into rat osteoarthritis knees. Biochem Biophys Res Commun. 2024;729: 150354.
10. Li M, Lu L, Xiao Q, Maalim AA, Nie B, Liu Y, Kahlert UD, Shu K, Lei T, Zhu M. Bioengineer mesenchymal stem cell for treatment of glioma by IL-12 mediated microenvironment reprogramming and nCD47-SLAMF7 mediated phagocytosis regulation of macrophages. Exploration. 2024. https://doi.org/10.1002/EXP.20240027.
11. Smolinska V, Debreova M, Culenova M, Csobonyeiova M, Svec A, Danisovic L. Implication of mesenchymal stem cells and their derivates for osteochondral regeneration. Int J Mol Sci. 2022;23(5):2490.
12. Maheshwer B, Polce EM, Paul K, Williams BT, Wolfson TS, Yanke A, Verma NN, Cole BJ, Chahla J. Regenerative potential of mesenchymal stem cells for the treatment of knee osteoarthritis and chondral defects: a systematic review and meta-analysis. Arthrosc J Arthrosc Relat Surg. 2021;37(1):362–78.
13. Koh Y-G, Kwon O-R, Kim Y-S, Choi Y-J. Comparative outcomes of open-wedge high tibial osteotomy with platelet-rich plasma alone or in combination with mesenchymal stem cell treatment: a prospective study. Arthrosc J Arthrosc Relat Surg. 2014;30(11):1453–60.
14. Wakitani S, Imoto K, Yamamoto T, Saito M, Murata N, Yoneda M. Human autologous culture expanded bone marrow mesenchymal cell transplantation for repair of cartilage defects in osteoarthritic knees. Osteoarthr Cartil. 2002;10(3):199–206.
15. Kim YS, Koh YG. Comparative matched-pair analysis of open-wedge high tibial osteotomy with versus without an injection of adipose-derived mesenchymal stem cells for varus knee osteoarthritis: clinical and second-look arthroscopic results. Am J Sports Med. 2018;46(11):2669–77.
16. Coryell PR, Diekman BO, Loeser RF. Mechanisms and therapeutic implications of cellular senescence in osteoarthritis. Nat Rev Rheumatol. 2021;17(1):47–57.
17. Ankrum JA, Ong JF, Karp JM. Mesenchymal stem cells: immune evasive, not immune privileged. Nat Biotechnol. 2014;32(3):252–60.
18. Pintore A, Notarfrancesco D, Zara A, Oliviero A, Migliorini F, Oliva F, Maffulli N. Intra-articular injection of bone marrow aspirate concentrate (BMAC) or adipose-derived stem cells (ADSCs) for knee osteoarthritis: a prospective comparative clinical trial. J Orthop Surg Res. 2023;18(1):350.
19. Le Blanc K, Tammik C, Rosendahl K, Zetterberg E, Ringdén O. HLA expression and immunologic properties of differentiated and undifferentiated mesenchymal stem cells. Exp Hematol. 2003;31(10):890–6.
20. Toma C, Wagner WR, Bowry S, Schwartz A, Villanueva F. Fate of culture-expanded mesenchymal stem cells in the microvasculature: in vivo observations of cell kinetics. Circ Res. 2009;104(3):398–402.
21. Zangi L, Margalit R, Reich-Zeliger S, Bachar-Lustig E, Beilhack A, Negrin R, Reisner Y. Direct imaging of immune rejection and memory induction by allogeneic mesenchymal stromal cells. Stem Cells. 2009;27(11):2865–74.
22. Caplan AI. Mesenchymal stem cells: time to change the name! Stem Cells Transl Med. 2017;6(6):1445–51.
23. Kim KI, Lee MC, Lee JH, Moon YW, Lee WS, Lee HJ, Hwang SC, In Y, Shon OJ, Bae KC, Song SJ, Park KK, Kim JH. Clinical efficacy and safety of the intra-articular injection of autologous adipose-derived mesenchymal stem cells for knee osteoarthritis: a phase III, randomized, double-blind, placebo-controlled trial. Am J Sports Med. 2023;51(9):2243–53.
24. Schumacher A, Mucha P, Puchalska I, Deptuła M, Wardowska A, Tymińska A, Filipowicz N, Mieczkowska A, Sachadyn P, Piotrowski A, Pikuła M, Cichorek M. Angiopoietin-like growth factor-derived peptides as biological activators of adipose-derived mesenchymal stromal cells. Biomed Pharmacother. 2024;177: 117052.
25. Lau CS, Park SY, Ethiraj LP, Singh P, Raj G, Quek J, Prasadh S, Choo Y, Goh BT. Role of adipose-derived mesenchymal stem cells in bone regeneration. Int J Mol Sci. 2024;25(12):6805.
26. Kostecka A, Kalamon N, Skoniecka A, Koczkowska M, Skowron PM, Piotrowski A, Pikuła M. Adipose-derived mesenchymal stromal cells in clinical trials: insights from single-cell studies. Life Sci. 2024;351: 122761.
27. Elzainy A, El Sadik A, Altowayan WM. Comparison between the regenerative and therapeutic impacts of bone marrow mesenchymal stem cells and adipose mesenchymal stem cells pre-treated with melatonin on liver fibrosis. Biomolecules. 2024;14(3):297.
28. Villanueva S, Carreño JE, Salazar L, Vergara C, Strodthoff R, Fajre F, Céspedes C, Sáez PJ, Irarrázabal C, Bartolucci J, Figueroa F, Vio CP. Human

mesenchymal stem cells derived from adipose tissue reduce functi onal and tissue damage in a rat model of chronic renal failure. Clin Sci. 2013;125(4):199–210.
29. Chang D, Fan T, Gao S, Jin Y, Zhang M, Ono M. Application of mesenchymal stem cell sheet to treatment of ischemic he art disease. Stem Cell Res Ther. 2021;12(1):384.
30. Li S, Zhang X, Liu M, Lu Q, Yu Y, Miao Z, Luo D, Han K, Li L, Qian W, Liu P. Not using a tourniquet is superior to tourniquet use for high tibial osteotomy: a prospective, randomised controlled trial. Int Orthop. 2022;46(4):823–9.
31. Li S, Yang J, Watson C, Lu Q, Zhang M, Miao Z, Luo D, Liu P. Drainage relieves pain without increasing post-operative blood loss in high tibial osteotomy: a prospective randomized controlled study. Int Orthop. 2020;44(6):1037–43.
32. Freitag J, Bates D, Wickham J, Shah K, Huguenin L, Tenen A, Paterson K, Boyd R. Adipose-derived mesenchymal stem cell therapy in the treatment of knee osteoarthritis: a randomized controlled trial. Regen Med. 2019;14(3):213–30.
33. Lee WS, Kim HJ, Kim KI, Kim GB, Jin W. Intra-articular injection of autologous adipose tissue-derived mesenchymal stem cells for the treatment of knee osteoarthritis: a phase IIb, randomized, placebo-controlled clinical trial. Stem Cells Transl Med. 2019;8(6):504–11.
34. Mainil-Varlet P, Aigner T, Brittberg M, Bullough P, Hollander A, Hunziker E, Kandel R, Nehrer S, Pritzker K, Roberts S, Stauffer E. Histological assessment of cartilage repair: a report by the Histology Endpoint Committee of the International Cartilage Repair Society (ICRS). J Bone Joint Surg. 2003;85-A(Suppl 2):45–57.
35. Casula V, Hirvasniemi J, Lehenkari P, Ojala R, Haapea M, Saarakkala S, Lammentausta E, Nieminen MT. Association between quantitative MRI and ICRS arthroscopic grading of articular cartilage. Knee Surg Sports Traumatol Arthrosc. 2016;24(6):2046–54.
36. Brittberg M, Winalski CS. Evaluation of cartilage injuries and repair. J Bone Joint Surg. 2003;85-A(Suppl 2):58–69.
37. Valdes AM, Doherty S, Muir KR, Zhang W, Maciewicz RA, Wheeler M, Arden N, Cooper C, Doherty M. Genetic contribution to radiographic severity in osteoarthritis of the knee. Ann Rheum Dis. 2012;71(9):1537–40.
38. Collins NJ, Misra D, Felson DT, Crossley KM, Roos EM. Measures of knee function: International Knee Documentation Committee (IKDC) Subjective Knee Evaluation Form, Knee Injury and Osteoarthritis Outcome Score (KOOS), Knee Injury and Osteoarthritis Outcome Score Physical Function Short Form (KOOS-PS), Knee Outcome Survey Activities of Daily Living Scale (KOS-ADL), Lysholm Knee Scoring Scale, Oxford Knee Score (OKS), Western Ontario and McMaster Universities Osteoarthritis Index (WOMAC), Activity Rating Scale (ARS), and Tegner Activity Score (TAS). Arthritis Care Res. 2011;63(Suppl 11):S208–28.
39. Dominici M, Le Blanc K, Mueller I, Slaper-Cortenbach I, Marini F, Krause D, Deans R, Keating A, Prockop D, Horwitz E. Minimal criteria for defining multipotent mesenchymal stromal cells. Int Soc Cell Ther Position Statement Cytother. 2006;8(4):315–7.
40. Gong W, Xu J, Wang Y, Min Q, Chen X, Zhang W, Chen J, Zhan Q. Nuclear genome-derived circular RNA circPUM1 localizes in mitochondria and regulates oxidative phosphorylation in esophageal squamous cell carcinoma. Signal Transduct Target Ther. 2022;7(1):40.
41. Hashimoto Y, Nishida Y, Takahashi S, Nakamura H, Mera H, Kashiwa K, Yoshiya S, Inagaki Y, Uematsu K, Tanaka Y, Asada S, Akagi M, Fukuda K, Hosokawa Y, Myoui A, Kamei N, Ishikawa M, Adachi N, Ochi M, Wakitani S. Transplantation of autologous bone marrow-derived mesenchymal stem cells under arthroscopic surgery with microfracture versus microfracture alone for articular cartilage lesions in the knee: a multicenter prospective randomized control clinical trial. Regen Ther. 2019;11:106–13.
42. Wong KL, Lee KBL, Tai BC, Law P, Lee EH, Hui JHP. Injectable cultured bone marrow-derived mesenchymal stem cells in varus knees with cartilage defects undergoing high tibial osteotomy: a prospective, randomized controlled clinical trial with 2 years' follow-up. Arthrosc J Arthrosc Relat Surg. 2013;29(12):2020–8.
43. Al-Najar M, Khalil H, Al-Ajlouni J, Al-Antary E, Hamdan M, Rahmeh R, Alhattab D, Samara O, Yasin M, Abdullah AA, Al-jabbari E, Hmaid D, Jafar H, Awidi A. Intra-articular injection of expanded autologous bone marrow mesenchymal cells in moderate and severe knee osteoarthritis is safe: a phase I /II study. J Orthop Surg Res. 2017;12(1):1–6.
44. Chahal J, Gómez-Aristizábal A, Shestopaloff K, Bhatt S, Chaboureau A, Fazio A, Chisholm J, Weston A, Chiovitti J, Keating A, Kapoor M, Ogilvie-Harris DJ, Syed KA, Gandhi R, Mahomed NN, Marshall KW, Sussman MS, Naraghi AM, Viswanathan S. Bone marrow mesenchymal stromal cell treatment in patients with osteoarthritis results in overall improvement in pain and symptoms and reduces synovial inflammation. Stem Cells Transl Med. 2019;8(8):746–57.
45. Goncars V, Jakobsons E, Blums K, Briede I, Patetko L, Erglis K, Erglis M, Kalnberzs K, Muiznieks I, Erglis A. The comparison of knee osteoarthritis treatment with single-dose bone marrow-derived mononuclear cells vs. hyaluronic acid injections. Medicina. 2017;53(2):101–8.
46. Koh Y-G, Kwon O-R, Kim Y-S, Choi Y-J, Tak D-H. Adipose-derived mesenchymal stem cells with microfracture versus microfracture alone: 2-year follow-up of a prospective randomized trial. Arthrosc J Arthrosc Relat Surg. 2016;32(1):97–109.
47. Lu L, Dai C, Zhang Z, Du H, Li S, Ye P, Fu Q, Zhang L, Wu X, Dong Y, Song Y, Zhao D, Pang Y, Bao C. Treatment of knee osteoarthritis with intra-articular injection of autologous adipose-derived mesenchymal progenitor cells: a prospective, randomized, double-blind, active-controlled, phase IIb clinical trial. Stem Cell Res Ther. 2019;10(1):1–10.
48. Pers Y-M, Rackwitz L, Ferreira R, Pullig O, Delfour C, Barry F, Sensebe L, Casteilla L, Fleury S, Bourin P, Noël D, Canovas F, Cyteval C, Lisignoli G, Schrauth J, Haddad D, Domergue S, Noeth U, Jorgensen C, on behalf of the ADIPOA Consortium. Adipose mesenchymal stromal cell-based therapy for severe osteoarthritis of the knee: a phase I dose-escalation trial. Stem Cells Transl Med. 2016;5(7):847–56.
49. Spasovski D, Spasovski V, Baščarević Z, Stojiljković M, Vreća M, Anđelković M, Pavlović S. Intra-articular injection of autologous adipose-derived mesenchymal stem cells in the treatment of knee osteoarthritis. J Gene Med. 2018;20(1): e3002.
50. Song Y, Du H, Dai C, Zhang L, Li S, Hunter DJ, Lu L, Bao C. Human adipose-derived mesenchymal stem cells for osteoarthritis: a Pilot study with long-term follow-up and repeated injections. Regen Med. 2018;13(3):295–307.
51. Kim YS, Choi YJ, Lee SW, Kwon OR, Suh DS, Heo DB, Koh YG. Assessment of clinical and MRI outcomes after mesenchymal stem cell implantation in patients with knee osteoarthritis: a prospective study. Osteoarthr Cartil. 2016;24(2):237–45.
52. Koh Y-G, Choi Y-J. Infrapatellar fat pad-derived mesenchymal stem cell therapy for knee osteoarthritis. Knee. 2012;19(6):902–7.
53. Kim YS, Choi YJ, Suh DS, Heo DB, Kim YI, Ryu J-S, Koh YG. Mesenchymal stem cell implantation in osteoarthritic knees. Am J Sports Med. 2015;43(1):176–85.
54. Turajane T, Chaveewanakorn U, Fongsarun W, Aojanepong J, Papadopoulos KI. Avoidance of total knee arthroplasty in early osteoarthritis of the knee with intra-articular implantation of autologous activated peripheral blood stem cells versus hyaluronic acid: a randomized controlled tri al with differential effects of growth factor addition. Stem Cells Int. 2017;2017:1–10.
55. Yoshida S, Nishitani K, Yoshitomi H, Kuriyama S, Nakamura S, Fujii T, Saito M, Kobori Y, Murakami A, Murata K, Ito H, Ueno H, Matsuda S. Knee alignment correction by high tibial osteotomy reduces symptoms and synovial inflammation in knee osteoarthritis accompanied by macrophage phenotypic change from M1 to M2. Arthritis Rheumatol. 2023;75(6):950–60.
56. Wu ZP, Zhang P, Bai JZ, Liang Y, Chen PT, He JS, Wang JC. Comparison of navigated and conventional high tibial osteotomy for the treatment of osteoarthritic knees with varus deformity: a meta-analysis. Int J Surg. 2018;55:211–9.
57. Niemeyer P, Schmal H, Hauschild O, von Heyden J, Südkamp NP, Köstler W. Open-wedge osteotomy using an internal plate fixator in patients with medial-compartment gonarthritis and varus malalignment: 3-year results with regard to preoperative arthroscopic and radiographic findings. Arthrosc J Arthrosc Relat Surg. 2010;26(12):1607–16.
58. Hernigou P, Roussignol X, Flouzat-Lachaniette CH, Filippini P, Guissou I, Poignard A. Opening wedge tibial osteotomy for large varus deformity with Ceraver resorbable beta tricalcium phosphate wedges. Int Orthop. 2010;34(2):191–9.
59. Xie J, Lin J, Wei M, Teng Y, He Q, Yang G, Yang X. Sustained Akt signaling in articular chondrocytes causes osteoarthritis via oxidative stress-induced senescence in mice. Bone Res. 2019;7:23.

60. Gao B, Lin X, Jing H, Fan J, Ji C, Jie Q, Zheng C, Wang D, Xu X, Hu Y, Lu W, Luo Z, Yang L. Local delivery of tetramethylpyrazine eliminates the senescent phenotype of bone marrow mesenchymal stromal cells and creates an anti-inflammatory and angiogenic environment in aging mice. Aging Cell. 2018;17(3): e12741.
61. Yu B, Ma J, Li J, Wang D, Wang Z, Wang S. Mitochondrial phosphatase PGAM5 modulates cellular senescence by regulating mitochondrial dynamics. Nat Commun. 2020;11(1):2549.
62. Upadhyay M, Milliner C, Bell BA, Bonilha VL. Oxidative stress in the retina and retinal pigment epithelium (RPE): role of aging, and DJ-1. Redox Biol. 2020;37: 101623.
63. Ma L, Feng X, Wang K, Song Y, Luo R, Yang C. Dexamethasone promotes mesenchymal stem cell apoptosis and inhibits osteogenesis by disrupting mitochondrial dynamics. FEBS Open Bio. 2020;10(2):211–20.
64. Wang T, Liu X, He C. Glucocorticoid-induced autophagy and apoptosis in bone. Apoptosis. 2020;25(3–4):157–68.
65. Sun Y, Li W, Lu Z, Chen R, Ling J, Ran Q, Jilka RL, Chen XD. Rescuing replication and osteogenesis of aged mesenchymal stem cells by exposure to a young extracellular matrix. FASEB J. 2011;25(5):1474–85.
66. Block TJ, Marinkovic M, Tran ON, Gonzalez AO, Marshall A, Dean DD, Chen XD. Restoring the quantity and quality of elderly human mesenchymal stem cells for autologous cell-based therapies. Stem Cell Res Ther. 2017;8(1):239.

## Publisher's Note